

Near-forward Raman study of a phonon-polariton reinforcement regime in the Zn(Se,S) alloy

RAMI HAJJ HUSSEIN¹, OLIVIER PAGÈS^{1(a)}, FRANCISZEK FIRSZT², AGNIESZKA MARASEK², WOJTEK PASZKOWICZ³, ALAIN MAILLARD⁴ and LAURENT BROCH¹

¹ LCP-A2MC, Institut Jean Barriol, Université de Lorraine, France

² Institute of Physics, N. Copernicus University, 87-100 Toruń, Poland

³ Institute of Physics, Polish Academy of Sciences, 02-668 Warsaw, Poland

⁴ LMOPS, Université de Lorraine – Sup'elec, 2, rue Edouard Belin, 57070 Metz, France

received and accepted dates provided by the publisher
other relevant dates provided by the publisher

PACS 63.20.-e – Phonons in crystal lattices
PACS 63.50.Gh – Disordered crystalline alloys
PACS 78.30.-j – Infrared and Raman spectra

Abstract – We investigate by near-forward Raman scattering a presumed reinforcement of the (A-C,B-C)-mixed phonon-polariton of a $A_{1-x}B_xC$ zincblende alloy when entering its longitudinal optical (LO -)regime near the Brillouin zone centre Γ , as predicted within the formalism of the linear dielectric response. A choice system to address such issue is $ZnSe_{0.68}S_{0.32}$ due to the moderate dispersion of its refractive index in the visible range, a *sine qua non* condition to bring the phonon-polariton insight near Γ . The LO -regime is actually accessed by using the 633.0 nm laser excitation, testified by the strong emergence of the (Zn-Se,Zn-S)-mixed phonon-polariton at ultimately small scattering angles.

Due to the polarity of the chemical bonding in such a ionic crystal as a zincblende AB semiconductor compound, the long-wavelength (Γ -like, $q \sim 0$) transverse optical (TO) phonon, corresponding to anti-phase displacement of the intercalated A-like and B-like *fcc* sublattices (mechanical character), is likely to be accompanied by a macroscopic electric field [1]. The latter is transversal to the direction of propagation, thus identical in nature to that carried by a pure electromagnetic wave, namely a photon. Now, due to the quasi vertical dispersion of a photon at the scale of the Brillouin zone, the electromagnetic character of a TO mode can only emerge very close to Γ . The concerned q values are of the order of one per ten thousands of the Brillouin zone size [2]. At this limit the electromagnetic and mechanical characters combine, conferring on a TO mode the status of a so-called phonon-polariton (PP). For certain q values the PP might acquire a dominant electromagnetic character, thus propagating at lightlike speeds. This stimulates interest in view of ultrafast

(photon-like) signal processing at THz (phonon-like) frequencies [3].

The ω vs. q dispersion of PP 's propagating in the bulk of various AB zincblende compounds have been abundantly studied, both experimentally and theoretically [2,4-9]. In a nutshell, it can be grasped within four asymptotic behaviors, i.e. two photon-like ones (ω -related) and two phonon-like ones (q -related). For large q values, i.e. falling within few percent of the Brillouin zone size, as routinely accessible in a conventional backscattering Raman experiment (schematically operating in a “reflection mode”, see below), a transverse electric field cannot propagate at THz (phonon-like) frequencies, because the considered (ω, q) -domain falls far away from the natural dispersion of a photon (quasi vertical). In such so-called q_∞ -regime, a TO mode thus reduces to a purely mechanical oscillator (abbreviated PM - TO hereafter, deprived of electric field), whose frequency, noted ω_{TO} , constitutes the first phonon-like asymptote, i.e. away from Γ . The frequency of the non-dispersive longitudinal optical (LO) mode, noted ω_{LO} , larger than ω_{TO} [10], defines the second phonon-like

^(a) Corresponding author

E-mail: olivier.pages@univ-lorraine.fr

asymptote, near Γ then, taking into account that the TO and LO modes are degenerate strictly at Γ [11]. Two remaining photon-like asymptotes determine limit PP -behaviors away from the $(PM-TO)-LO$ resonance, as dictated by the static ϵ_0 ($\omega > \omega_{TO}$) and high-frequency ϵ_∞ ($\omega \gg \omega_{TO}$) relative dielectric constants of the crystal. The strong PP coupling occurs when the quasi vertical photon-like asymptotes cross the horizontal TO and LO phonon-like ones. This gives rise to an anticrossing, resulting in two distinct PP branches. The upper branch is phonon-like (LO) when $q \rightarrow 0$ and photon-like ($\omega = q \times c \times \epsilon_\infty^{-1}$ where c represents the speed of light in vacuum) at $\omega \gg \omega_{TO}$, while the lower branch is photon-like ($\omega = q \times c \times \epsilon_0^{-1}$) at $\omega \ll \omega_{TO}$ and phonon-like in the q_∞ -regime ($PM-TO$). Note that the $(PM-TO)-LO$ band is forbidden for the propagation of bulk PP 's, only surface PP 's can propagate therein.

An interesting question is how such PP picture modifies for a multi-oscillator system such as a $AB_{1-x}C_x$ zincblende alloy (A standing for a cation or an anion)? Bao and Liang provided a pioneering theoretical insight into the ' ω vs. q ' PP -dispersion of various $AB_{1-x}C_x$ zincblende alloys [12,13]. As a starting point they assumed a crude two-mode [$1 \times (A-C), 1 \times (A-C)$] $PM-TO$ pattern behind the PP 's, as explained within the modified-random-element-isodisplacement (MREI) model [14]. Besides the lower and upper alloy-related branches, assimilating to those of a pure compound as described above [2,4-9], an intermediary (A-C, B-C) - mixed PP was predicted by Bao and Liang. The latter branch is distinct in nature from the former parent-like two in that it exhibits an overall S-like shape governed by two phonon-like asymptotes only, i.e. the higher $PM-TO$ frequency in the q_∞ -regime, say the BC-like one, and the lower LO frequency near Γ , the AC-like one then [12,13]. As such, its dispersion covers the gap between the natural A-C and B-C vibration frequencies, possibly a considerable one depending on the alloy.

We have refined the above PP -picture at the occasion of a recent near-forward Raman study (schematically operating in a "transmission mode", see below) of the $Zn_{0.67}Be_{0.33}Se$ zincblende alloy characterized by a three-mode [$1 \times (Zn-Se), 2 \times (Be-Se)$] $PM-TO$ pattern in the q_∞ -regime. Such three-mode pattern falls beyond the scope of the MREI scheme. It was explained by introducing the phenomenological percolation model [15]. In brief, this model distinguishes between the vibrations of the short (Be-Se) bonds depending on whether their local environment is more rich of one or the other (Zn-Se or Be-Se) species (1-bond \rightarrow 2-mode behavior) [16]. At this occasion, two intermediary (Zn-Se, Be-Se)-mixed PP 's were revealed, and not only one as predicted within the MREI scheme. Each intermediary PP relates to a particular BeSe-like $PM-TO$ in the q_∞ -regime, and collapses with an S-like shape onto the LO immediately underneath near Γ , consistently with

the basic MREI trend (see above). In particular, the lower-intermediary PP , noted PP^- , attracts attention, for two reasons. First, in contrast with the upper-intermediary PP , noted PP^+ , which remains confined within the upper doublet of $PM-TO$'s (BeSe-like in this case), PP^- may exhibit a considerable dispersion, as discussed above within the MREI scheme. Second, as soon as entering the PP regime, PP^- becomes much dominant over PP^+ .

The q -dependence of the PP^- Raman intensity constitutes *per se* an interesting issue. Based on our recent near-forward Raman study of $Zn_{0.67}Be_{0.33}Se$ limited to the early stage of the PP regime (a moderate PP^- red-shift of $\sim 15 \text{ cm}^{-1}$ was detected, representing less than ten percent of the total PP^- dispersion), we already know that the initial q -induced softening of PP^- goes with a progressive collapse of this mode [15]. Now, as PP^- is supposed to assimilate to a LO near Γ [12,13,15], *a priori* showing up strong and sharp in the Raman spectrum, we anticipate that, after its initial collapse, PP^- should reinforce. This points to a specific PP feature of an alloy, yet unexplored, neither experimentally nor theoretically.

In this work we tackle such issue both theoretically, within the formalism of the linear dielectric response, and experimentally, by applying the near-forward Raman scattering to the $ZnSe_{0.68}S_{0.32}$ zincblende alloy. Due to large optical gaps of ZnSe (2.7 eV) and ZnS (3.6 eV) [17], $ZnSe_{0.68}S_{0.32}$ is transparent to visible laser lines, thus well-suited in view of a near-forward Raman study. Besides, the frequency gap between the $PM-TO$'s of its (Zn-Se and Zn-S) constituting bonds is narrow ($235-285 \text{ cm}^{-1}$, see below), with concomitant impact on the magnitude of the PP^- dispersion. This offers an opportunity to explore the PP^- dispersion in a different context than was earlier done with $Zn_{0.67}Be_{0.33}Se$ [15], the latter alloy being characterized by a huge PP^- dispersion ($250 - 450 \text{ cm}^{-1}$). Basically, our aim is to penetrate deep into the PP^- dispersion of $ZnSe_{0.68}S_{0.32}$ so as to address minimal q values likely to fall into the LO -regime of PP^- , near Γ .

Generally, the wavevector q of a TO mode (a PP one near Γ or the corresponding $PM-TO$ one in the q_∞ -regime) accessible in a Raman experiment is governed by the conservation rule $q = k_i - k_s$ in which k_i and k_s are the wavevectors of the incident laser beam and of the scattered light, respectively, both taken inside the crystal, forming an angle θ . In a standard backscattering geometry k_i and k_s are (nearly) antiparallel ($\theta \sim 180^\circ$), so that q is maximum, falling deep into the q_∞ -regime. Minimum q values, i.e. those likely to address the PP -regime, are achieved by taking k_i and k_s (nearly) parallel ($\theta \sim 0^\circ$), using a near-forward Raman setup. From the above conservation rule,

$$q = c^{-1} \times \{n^2(\omega_i, x) \times \omega_i^2 + n^2(\omega_s, x) \times \omega_s^2\}$$

$$-2 \times n(\omega_i, x) \times n(\omega_s, x) \times \omega_i \times \omega_s \times \cos \theta \}^{0.5} \quad (1)$$

where ω_i and ω_s are the frequencies of the incident and scattered lights, respectively, and $n(\omega_i, x)$ and $n(\omega_s, x)$ the corresponding refractive indexes of the considered $AB_{1-x}C_x$ alloy. If we refer to pure ZnSe and pure ZnS, the refractive index of $ZnSe_{1-x}S_x$ is expected to decrease with the frequency in the visible range. Accordingly one cannot achieve $q=0$ (Γ) in practice. Indeed the minimum q value, accessed in a perfect forward scattering experiment ($\theta \sim 0^\circ$), i.e. $q_{min} = |n(\omega_i) \times \omega_i - n(\omega_s) \times \omega_s|$, remains finite because the difference in frequencies is augmented by the difference in refractive indexes. Optimum conditions are thus reached by minimizing the dispersion of the refractive index around the used laser excitation. The alloy composition ($ZnSe_{0.68}S_{0.32}$) as well as the laser excitation (ω_i) used, were selected in this spirit, as discussed below.

The $ZnSe_{0.68}S_{0.32}$ sample considered in this work was grown from the melt as a single crystal (cylinder, ~ 3 mm-high and ~ 8 mm in diameter) by using the high-pressure Bridgman method (see detail, e.g. in Ref. [18]). The near-forward and backward Raman spectra are taken along the [110]-growth axis, corresponding to a nominal (TO -allowed, LO -forbidden) geometry, after optical polishing of the opposite (110) faces to optical quality until quasi parallelism was achieved.

The selected alloy corresponds to the highest achievable S incorporation by the Bridgman method. This provides optimal conditions with respect to the dispersion of the refractive index, since the latter is larger for ZnSe than for ZnS in the visible range [19]. In fact, the wavelength (λ) dependence of the $ZnSe_{0.68}S_{0.32}$ refractive index (n) measured by ellipsometry in the λ -range 450 – 770 nm (not shown), can be accurately fitted to the Cauchy dispersion formula

$$n(\lambda) = X + Y \times \lambda^2 \times 10^4 + Z \times \lambda^{-4} \times 10^9 \quad (2)$$

using (X, Y, Z) values of (3.1638 ∓ 0.0007 , 1.2380 ∓ 0.0536 , 14.0485 ∓ 0.1056), where X is dimensionless, Y and Z are constants with units of nm^2 and nm^4 , respectively, and λ is in nm . The minimum dispersion of the $ZnSe_{0.68}S_{0.32}$ refractive index is further achieved by shifting the Raman analysis to the less energetic end of the visible spectral range. We accordingly use the 633.0 nm line from a He-Ne laser to record the $ZnSe_{0.68}S_{0.32}$ near-forward Raman spectra, instead of the 514.5 nm and 488.0 nm Ar+ ones earlier used with $Zn_{0.67}Be_{0.33}Se$ [15], notwithstanding its inferior Raman efficiency. Along the same line, the Stokes experiment ($\omega_i > \omega_s$) was preferred against the anti-Stokes one ($\omega_i < \omega_s$), not to mention that the Stokes process is, further, more efficient.

Preliminary insight as to whether there is any

chance to access experimentally the presumed LO -like PP^- reinforcement with $ZnSe_{0.68}S_{0.32}$ in a near forward Raman scattering experiment using the 633.0 nm laser excitation is achieved by calculating the related multi- PP near-forward Raman cross section (RCS) in its (q, θ)-dependence. For doing so we use the generic RSC expression established in Ref. [15], which we reproduce hereafter in its specific form applying to multi- PP 's propagating in the bulk of an alloy containing p oscillators (in reference to the multi $PM-TO$'s of the q_∞ -regime behind the PP 's),

$$RCS(\omega, q, x) \sim \text{Im} \{ -[\epsilon_r(\omega, x) - q^2 c^2 \omega^{-2}]^{-1} \times [1 + \sum C_p(x) L_p(\omega, x)]^2 + \sum C_p^2(x) \omega_p^2(x) L_p(\omega, x) S_p^{-1}(x) \epsilon_{\infty, p}^{-1} \omega_p^{-2} \} \quad (3)$$

$\epsilon_r(\omega, x)$ is the relative dielectric function of the $AB_{1-x}C_x$ alloy taken in its classical form, including the electronic contribution, $\epsilon_\infty(x)$, varying linearly with x between the parent values, and a summation over the p ionic oscillators present in the crystal, each represented by a damped Lorentzian resonance $L_p(\omega, x) = \omega_p^2(x) \times (\omega_p^2(x) - \omega^2 - j \times \gamma_p(x) \times \omega)$ at the relevant $PM-TO$ frequency $\omega_p(x)$ in the q_∞ -regime. The damping parameter $\gamma_p(x)$ is sample-dependent. $C_p(x)$ and $S_p(x)$ are the p -related Faust-Henry coefficient and oscillator strength, monitoring the Raman intensity and the ($PM-TO$)- LO frequency gap of oscillator p , respectively. Both parameters scale linearly with the fraction of oscillator p in the crystal. The ($C_p, S_p, \omega_p, \epsilon_{\infty, p}$) values of the pure ZnSe or ZnS compound related to oscillator p are ($-0.7, 2.92, 254.5 \text{ cm}^{-1}, 5.75$) [15] and (-0.45 [20], 2.57 [21], 277.0 cm^{-1} [22], 5.20 [22]), respectively. Remaining alloy-related input parameters are the number p of oscillators *per* alloy, the corresponding $\omega_p(x)$ frequencies and the fractions $f_p(x)$ of such oscillators at a given composition x . Such [$p, \omega_p(x), f_p(x)$] parameters refer to the q_∞ -regime, and are thus accessible from a pure- TO backscattering Raman insight or by infrared absorption.

Vinogradov *et al.* have revealed a three-mode [$1 \times (Zn-Se), 2 \times (Zn-S)$] $PM-TO$ pattern for $ZnSe_{1-x}S_x$ ($p=3$) in their recent exhaustive infrared study [22]. The question as to whether the Zn-S doublet falls into the scope of the 1-bond \rightarrow 2-mode percolation scheme or not will be debated elsewhere. For our present use we may only retain that the two Zn-S $PM-TO$'s, presently labelled as $TO_{Zn-S,1}$ and $TO_{Zn-S,2}$ show up distinctly in the backscattering Raman spectrum of $ZnSe_{0.68}S_{0.32}$, being characterized by comparable Raman intensities (a direct insight is given below). This means that the available Zn-S oscillator strength, which scales as the Zn-S bond fraction, equally shares between the two Zn-S sub-modes, leading to $f_{Zn-S,1} = f_{Zn-S,2} = 0.16$. As for the unique Zn-Se mode, its oscillator strength directly scales as the Zn-Se bond fraction, so that $f_{Zn-Se} = 0.68$. Last, the three [$TO_{Zn-Se}, TO_{Zn-S,1}, TO_{Zn-S,2}$] $PM-TO$'s emerge at the $\omega_p(x)$

the LO_{Zn-Se} and LO_{Zn-S^+} modes at ~ 245 and ~ 322 cm^{-1} , respectively, and also the so-called A-band around 165 cm^{-1} , reflecting the acoustical two-phonon density of states. We mention that the emergence of theoretically forbidden optic modes or acoustic bands is a common feature of alloys, due to a partial breaking of the wavevector conservation rule by the alloy disorder. As for the minor LO_{Zn-S^-} mode of the Zn-S doublet [15,16], this remains screened by the related $PM-TO$'s nearby (see Fig. 1). Satisfactory contour modeling of the nominal three-mode $PM-TO$ pattern (top thin curve in Fig. 2) is achieved both in the Zn-Se (not shown) and Zn-S (thin line) spectral ranges by injecting our above selection of input parameters into the asymptotic form of Eq. (3) valid in the q_∞ -regime (backscattering-like), in fact reduced to its second term, taking the same $\gamma_p(x)$ damping of 24 cm^{-1} for the two Zn-S sub-modes.

Now we change the Raman setup from backscattering to near-forward scattering. A representative series of near-forward Raman spectra taken at different θ angles with respect to the [110]-growth axis of the $ZnSe_{0.68}S_{0.32}$ ingot using the 633.0 nm laser line are shown in Fig. 2 (thin spectra). The intensities, normalized to the θ -insensitive A-band, are directly comparable. In each spectrum the near-forward Raman signal (PP^- -labeling in Figs. 1 and 2) is partially obscured by the θ -insensitive backscattering one (TO -labeling in abbreviation of $PM-TO$) generated after reflection of the laser beam at the top surface (detector side) of the sample. As PP^+ is located within the Zn-S doublet of parasitical $PM-TO$'s (see Fig. 1), it remains screened at any angle, only PP^- , falling outside the doublet, is visible. Its (q, θ) -dependence is discussed hereafter.

The relevant θ angle per spectrum (see Fig. 2) is determined by adjusting the frequency of the theoretical PP^- peak obtained by Eq. (3) to the experimental frequency. As long as θ is larger than $\sim 4.0^\circ$, the near-forward Raman signal of $ZnSe_{0.68}S_{0.32}$ remains stable, similar to the reference backscattering one ($\theta \sim 180^\circ$). Below this critical angle, the multi- TO 's enter their PP -regime, signed by the red-shift of PP^- (see arrows in Fig. 2). Note that the minimum achievable θ angle remains finite ($\sim 0.3^\circ$), meaning that the near-forward Raman study cannot be fully developed in practice. This, we attribute to slight k_i^- -disorientations inside the crystal due to inherent defects in an alloy. Nevertheless, the accessible θ -domain suffices to reach the LO -like reinforcement regime ($\theta : 1.0^\circ \rightarrow 0.3^\circ$) beyond the initial collapse regime ($\theta : 4.0^\circ \rightarrow 1.3^\circ$, see Figs. 1 and 2), testified by the development of PP^- into a sharp and intense feature at near-normal incidences. Fair contour modeling of the peak PP^- at the minimum achievable θ angle ($\sim 0.3^\circ$) is obtained by using the same input parameters as specified above, taking a reduced damping of 12 cm^{-1} . We emphasize that the backscattering ($PM-TO$'s abbreviated TO 's, upper thin curve in Fig. 2) and near-

forward (PP^- , lower thin curve) theoretical signals are directly comparable. Incidentally, we have checked that a similar near-forward Raman study with $Zn_{0.67}Be_{0.33}Se$ (see Ref. [15]) using the 633.0 nm laser excitation falls short of engaging the PP^- reinforcement regime, due to an unfavorable dispersion of the refractive index.

Last, we discuss briefly the Zn-Se signal. At first sight it remains θ -insensitive, pinned by a Fano interference with the A-band nearby (a characteristic antiresonance is marked by an asterisk in Fig. 2), as earlier discussed for $Zn_{0.67}Be_{0.33}Se$ [15]. The dramatic weakening of the near-forward Zn-Se signal with respect to the backscattering one (divided by ~ 5 , see Fig. 2) is attributed to a reinforcement of the Fano interference that occurs when the Zn-Se mode engages its PP regime and starts to red-shift towards the θ -insensitive A-band. Now, a careful examination reveals that the Zn-Se line develops an increasing asymmetry on its low-frequency side when θ reduces, eventually disappearing at near-normal incidences. In the process, the Raman intensity reduces dramatically. A comparison with the reference A-band is explicit with this respect. The discussion of the appearance and then disappearance of such asymmetrical broadening under θ reduction, presumably related to some fine structuring of the ZnSe-like PP , falls beyond the scope of this work.

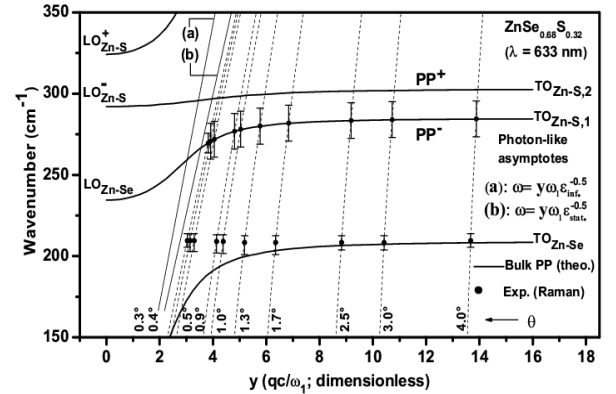


Fig. 3: Comparison between the theoretical and experimental ' ω vs. q ' multi- PP dispersions of $ZnSe_{0.68}S_{0.32}$, as obtained via Eq. (3) (thick lines) and by near-forward Raman scattering (symbols with error bars representing the Raman linewidths at half height), respectively. No experimental data is reported for PP^+ due to a screening at any θ angle. The relevant ' θ vs. y ' correspondences per Raman spectrum, in reference to Eq. (1), are added (refer to the oblique-hatched lines), for sake of completeness. The phonon asymptotes in the q_∞ -regime (TO labeling in abbreviation of $PM-TO$'s) and near Γ (LO labeling), together with the photon ones (thin lines) far-below (a) and far beyond (b) the phonon resonance are also specified, for reference purpose.

For sake of completeness, we provide in Fig. 3 a comparison between the theoretical (thin curves) and

experimental (symbols) ‘ ω vs. q ’ multi- PP dispersions of $\text{ZnSe}_{0.68}\text{S}_{0.32}$, as obtained via Eq. (3) – in reference to Fig. 1, and by near-forward Raman scattering – in reference to Fig. 2, respectively.

Summarizing, we perform a near-forward Raman study of the three-mode $[1 \times (\text{Zn-Se}), 2 \times (\text{Zn-S})]$ $\text{ZnSe}_{0.68}\text{S}_{0.32}$ alloy in search of the presumed LO -like reinforcement of the $(\text{Zn-Se}, \text{Zn-S})$ -mixed PP^- near Γ . The laser excitation as well as the alloy compositions were selected so as to minimize the dispersion of the refractive index, a prerequisite to penetrate deep into the PP^- dispersion in view to address the vicinity of Γ . The LO -regime is successfully accessed, as evidenced by the development of PP^- into a giant feature at ultimately small scattering angles, solving the raised issue in the positive sense. The discussion is supported by a contour modeling of the $\text{ZnSe}_{0.68}\text{S}_{0.32}$ multi- PP near-forward Raman lineshapes in their (q, θ) -dependence within the formalism of the linear dielectric response.

We would like to thank P. Franchetti and J.-P. Decruppe for technical assistance in the Raman measurements, C. Jobart for sample preparation, and A.V. Postnikov for useful discussions and careful reading of the manuscript. This work has been supported by the “Fonds Européens de DEveloppement Régional” of Region Lorraine (FEDER project N°. 34619).

REFERENCES

- [1] BORN M. and HUANG K., in *Dynamical Theory of Crystal Lattices* (Oxford University Press, Clarendon) 1954.
- [2] HENRY C. H. and HOPFIELD J. J., *Phys. Rev. Lett.* **15** (1965) 964.
- [3] STOYANOV N. S. *et al.*, *Nature Materials* **1** (2002) 95.
- [4] PORTO S. P. S., TELL B. and DAMEN T. C., *Phys. Rev. Lett.* **16** (1966) 450.
- [5] MARSCHALL N. and FISCHER B., *Phys. Rev. Lett.* **28** (1972) 811.
- [6] EVANS D. J., USHIODA S. and McMULLEN J., *Phys. Rev. Lett.* **31** (1973) 369.
- [7] MILLS D. L. and MARADUDIN A. A. *Phys. Rev. Lett.* **31** (1973) 372.
- [8] MILLS D. L. and BURSTEIN E., *Rep. Prog. Phys.* **37** (1974) 817.
- [9] WATANABE J.-I., UCHINOKURA K. and SEKINE T., *Phys. Rev. B* **40** (1989) 7860.
- [10] In contrast with the TO -like electric field, the LO -like electric field suffers no q -restriction, and remains invariant (non-dispersive) in between Γ and the q_∞ -regime. Therefore at this limit the effective force constant of the LO mode is reinforced by a coulombian contribution with respect to the purely-mechanical force constant of the TO mode, meaning that $\omega_{LO} > \omega_{TO}$.
- [11] For a given optical mode at Γ , one may as well consider that the wavevector, nul in fact, is oriented along the atom vibration (LO) or perpendicular to it (TO).
- [12] BAO J. and LIANG X. X., *J. Phys.: Condes. Matter* **18** (2006) 8229.
- [13] BAO J. and LIANG X. X., *J. Appl. Phys.* **104** (2008) 033545.
- [14] CHANG I. F. and MITRA S. S., *Phys. Rev.* **172** (1968) 924.
- [15] HAJJ HUSSEIN *et al.*, *Appl. Phys. Lett.* **103** (2013) 071912.
- [16] PAGÈS O. *et al.*, *Phys. Rev. B* **86** (2012) 045201.
- [17] DEVLIN S. S., in *Physics and Chemistry of II-VI Compounds*, edited by AVEN M. and PRENER J. S. (North Holland Publishing Company, Amsterdam) 1967, p. 603.
- [18] FIRSZT F. *et al.*, *Cryst. Res. Technol.* **40** (2005) 386.
- [19] LI H. H., *J. Phys. Chem. Ref. Data* **13** (1984) 103.
- [20] This value was adjusted so as to best reproduce the relative intensity ratio between the Zn-Se and Zn-S signals in the reference Raman spectrum of $\text{ZnSe}_{0.68}\text{S}_{0.32}$ taken in the backscattering geometry (see Fig. 2, top curve).
- [21] Value linearly extrapolated for pure ZnS from best adjustment of the ‘Zn-S oscillator strength vs. x’ experimental data reported at moderate S content for $\text{ZnSe}_{1-x}\text{S}_x$ in Ref. 22 (see Fig. 5 therein).
- [22] VINOGRADOV *et al.*, *Phys. Sol. State* **48** (2006) 1940.